Fabrication of Tin and Zinc Gas Diffusion Electrodes for Electrochemical Reduction of Carbon Dioxide

R. M. H. H. Jayarathne* iD, A. R. Nihmiya*† iD, A. H. L. R. Nilmini** iD and P. K. D. D. P. Pitigala***

*Department of Civil and Environmental Technology, Faculty of Technology, University of Sri Jayewardenepura, Homagama, Sri Lanka

**Department of Materials and Mechanical Technology, Faculty of Technology, University of Sri Jayewardenepura, Homagama, Sri Lanka

***Department of Physics, Faculty of Applied Sciences, University of Sri Jayewardenepura, Nugegoda, Sri Lanka

†Corresponding author: A.R. Nihmiya; nihmiya@sjp.ac.lk

ABSTRACT

This study explores the electrochemical reduction of carbon dioxide (CO_2) using tin (Sn) and zinc (Zn) catalyst-loaded gas diffusion electrodes (GDEs). The research explores the influence of electrolytic potential and catalyst loading on the efficiency of CO_2 conversion to valuable chemicals, specifically formic acid and carbon monoxide. The best Sn loading for Sn-loaded GDEs, according to the morphological study, is 7 mg.cm^{-2}, which results in higher current density (0.33 mA.cm^{-2}) and current efficiency (36%). An electrolytic potential of -1.3 V Vs. Ag/AgCl is identified as optimal for Sn GDEs, offering a balance between high current efficiency (35%) and controlled current density. For Zn-loaded GDEs, an optimal loading of 5 mg.cm^{2-} yields the highest current efficiency of 19.4% and a peak current density of 0.28 mA.cm^{2-} at an electrolytic potential of -1.55 V Vs. Ag/AgCl, in addition to highlighting the crucial role that catalyst loading and electrolytic potential play in enhancing CO_2 reduction efficiency, this research offers insightful information for environmentally friendly CO_2 conversion technology.

INTRODUCTION

The electrochemical reduction of carbon dioxide (ERC) has emerged as a promising and innovative approach to addressing two critical global challenges simultaneously: mitigating the rising levels of atmospheric CO_2 and producing valuable chemicals and fuels sustainably. The process of converting CO_2 to more useful chemicals, particularly "CO_2 neutral fuels," by using electrical energy is known as the electrochemical reduction of CO_2 (ERC). The ERC process occurs in an electrochemical cell (Fig. 1) at the interface of an electron conductor (cathode) and an ionic conductor (electrolyte). The ERC process involves a water oxidation reaction at the anode and a CO_2 reduction reaction at the cathode. As ERC consumes less energy than traditional chemical reduction processes and can proceed at a moderate temperature and atmospheric pressure, many researchers have proclaimed that ERC in large-scale applications is economically feasible. The economic feasibility of ERC intensely depends on the cathode, including its electrochemical performance and cost (Lu et al. 2014).

Most of the current cathodes for ERC are metal electrodes, and CO_2 is thus provided by sparging in the bulk. Carbon dioxide is introduced into the system by sparging it in the bulk solution. However, the efficiency of the ERC process is limited because CO_2 has low solubility in water at ambient conditions. This limitation arises from the challenge of transferring CO_2 effectively from the bulk solution to the cathode surface. To enhance the efficiency of ERC, gas diffusion electrodes (GDEs) have been developed. A GDE is a porous composite electrode consisting of a gas diffusion layer (GDL), a current collector (CC), and a catalyst layer (CL). The GDL serves the dual purpose of delivering gas and providing waterproofing. The CC is essential for reducing the ohmic losses in the electrode. The CL contains a gas-liquid-solid three-phase interface (TPI), which acts as the site for the ERC reaction.

This electrochemical process involves the use of electrodes and electrocatalysts to drive the conversion of CO_2 into a range of useful compounds, including formic acid (HCOOH), carbon monoxide (CO), methane (CH_4), and ethylene (C_2H_4) (Hori et al. 1989, Hori 2008). Through
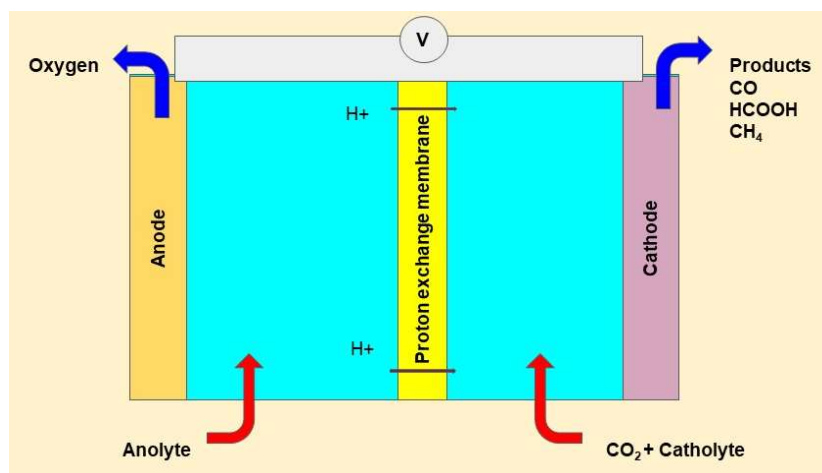
Fig. 1: Electrochemical cell mechanism.

careful control of reaction conditions and catalyst materials, researchers are exploring ways to optimize product selectivity and maximize energy efficiency. The field has witnessed significant advancements in recent years, with the development of novel catalysts, improved reactor designs, and a deeper understanding of reaction mechanisms.

The electrochemical reduction of CO_2 holds immense promise for sustainable energy storage, carbon capture and utilization, and the reduction of greenhouse gas emissions. In this context, this paper explores the fabrication of gas diffusion electrodes, particularly focusing on tin and zinc-based electrodes, as critical components in the electrochemical reduction of carbon dioxide.

Researchers have extensively investigated the use of Sn-based catalysts due to their remarkable activity and selectivity toward formic acid production (Del Castillo et al. 2017, Lei et al. 2018, Wang et al. 2021, Lee et al. 2015). Furthermore, Zn GDEs were also studied by researchers in the conversion of CO_2 to CO (Luo et al. 2019, Luo et al. 2020). Zn is an earth-abundant metal, reducing CO_2 to CO with relatively lower activity than Ag and Au catalysts. Because of the high cost and low abundance, Zn is better than Au and Au as catalysts (Jeanty et al. 2018, Chen et al. 2022, Shi et al. 2020).

A wide range of faradic efficiencies has been reported for formic acid formation on Sn electrodes. By using Sn GDE, Wang et al. (2014) obtained the highest Faradic efficiency of 72.99% and current density of 13.45 mA.cm^{-2} with Potassium Bicarbonate ($KHCO_3$) as the electrolyte. Del Castillo et al. (2017) obtained 70% Faradaic Efficiency and 150 mA.cm^{-2} current density with a low catholyte flow rate using Sn/C-GDEs. Luo et al. (2019) obtained 91.6%

CO faradaic efficiency with 200 mA.cm^{-2} current density at only -0.62 V vs RHE in a flow cell reactor.

In the ERC, the catalyst loading plays a pivotal role, directly influencing the efficiency and selectivity of the reaction. Researchers have extensively investigated the impact of varying catalyst concentrations, shedding light on the intricate balance between active sites and overcrowding, ultimately shaping the catalytic performance in CO_2 reduction processes. Studies reveal that the performance of Sn-based catalysts is significantly influenced by Sn loading (Wang et al. 2014, Del Castillo et al. 2015).

Understanding the influence of electrolytic potential is paramount in unraveling the complexities of electrochemical CO_2 reduction. Different potential levels profoundly impact the reaction kinetics, driving forces, and selectivity, offering a nuanced insight into the efficiency of CO_2 conversion processes. The effect of the electrolytic potential was studied by many researchers (Kim et al. 2014). Wu et al. (2014) studied about effects of the electrolytic potential for ERC with Sn electrode to obtain a high production for formic acid, and Luo et al. (2019) Studied the effect of electrolytic potential for Zn foil and Porous Zn electrode where CO_2 reduced to CO.

In this comprehensive study, we have delved deep into the intricate world of electrochemical reduction of carbon dioxide using tin (Sn) and zinc (Zn) loaded gas diffusion electrodes. The paper describes the electrochemical process, where CO_2 is transformed into valuable compounds, including formic acid and carbon monoxide, employing specialized electrocatalysts and electrodes. Through a systematic approach, we studied the influence of catalyst loading and electrolytic potential. The performance of electrolysis was evaluated using current density and current efficiency.

MATERIALS AND METHODS

Materials

Vulcan XC 72R Carbon Black Powder, polytetrafluoroethylene (PTFE) Dispersion 30(TE3970 type), Fumasep FAB-PK-130 (anion exchange membrane), EPDM Rubber sheet, were purchased from Fuel Cell Store. Nafion PFSA polymer dispersion D520 (5%), Ethanol, copper mesh, and stainless-steel mesh were purchased from the local market. Distilled water, Potassium Bicarbonate AR, 99.5%, Propan-2-ol 99.8% Tin metal powder pure 99%, and Zinc metal powder, 99% were used.

Methodology

Fabrication of gas diffusion electrodes: First, the mixture of conductive carbon black and ethanol was agitated ultrasonically for 2-3 min. Then polytetrafluoroethylene (PTFE) was added and further agitated ultrasonically and stirred in a hot bath for 10-12 min. Then, the dough was formed and rolled down to a thin film on a stainless-steel mesh to form a gas diffusion layer (GDL). For the preparation of the microporous layer, carbon black loading 25 mg.cm^{-2}, 5 mg.cm^{-2} PTFE and 5 mL of ethanol were used. The size of the GDEs made was 2×2 cm^2.

The Sn catalyst ink and Zn catalyst were made by mixing Sn and Zn catalyst particles separately, Nafion ionomer, isopropanol, and deionized water followed by ultrasonication of the mixture for 1 h. The amount of water to isopropanol is 1:1 in the mixture. The catalyst layer of the gas diffusion electrode was prepared by spraying the Sn-catalyst ink and Zn-catalyst on the rolling pressed GDL in several layers using the airbrush and mini compressor. Catalyst ink was sprayed in different loadings (3,5,7, and 9 mg.cm^{-2} with the same fraction of 50% wt. Nafion) on GDLs to make GDEs. The amount of deposited catalyst was detected by weighing.

Characterization of GDEs

Scanning electron microscopy (SEM) images of the GDEs were acquired using the ZEISS EVO 18 Scanning Electron Microscope.

Experimental setup for electrochemical testing: Electrolysis and EIS were carried out in a Corrtest CS310 Potentiostat/Galvanostat (Wuhan Corrtest Instruments Corp., Ltd., Wuhan, China) electrochemical workstation at room temperature in a three-compartment electrochemical cell. The working electrode was the fabricated GDE, and the copper mesh was the counter electrode, while Ag/AgCl was used as the reference electrode. An anion exchange membrane separated the cathode compartment and anode compartment. The electrolyte was circulated through the compartment using the peristaltic pump (Kamoer Fluid Tech (Shanghai) Co., Ltd). The anion exchange membrane was submerged in KOH solution for 6 to 12 h and then into potassium bicarbonate solution for a period of 48-72 to fully convert the membrane into bicarbonate form. After rinsing the membrane (which is in the carbonate form) with deionized water or distilled water, it was assembled inside the electrochemical setup for electrochemical CO_2 reduction experiments.

Gas products were collected in gas sampling bags (Aluminum foil gas sampling bags, Guangzhou Huaixing Technology Co., Ltd., China), while liquid products to glass bottles. CO_2 was fed into the gas inlet continuously throughout the experiment. Fig. 1 shows the configuration

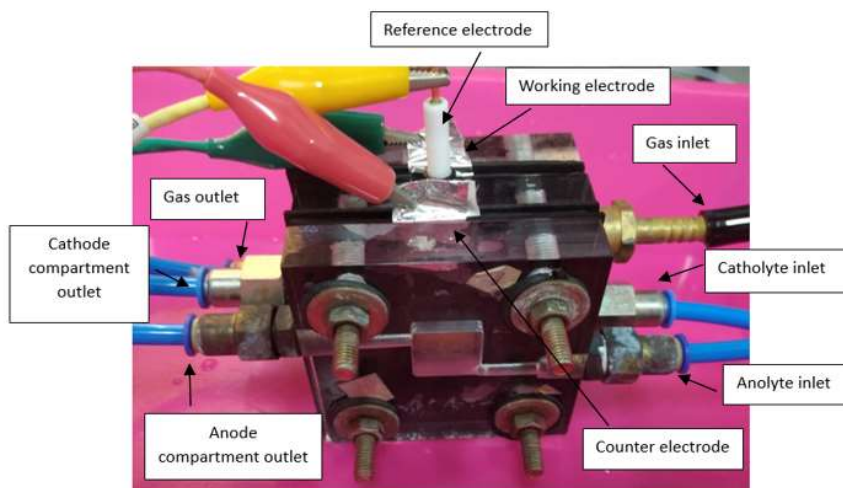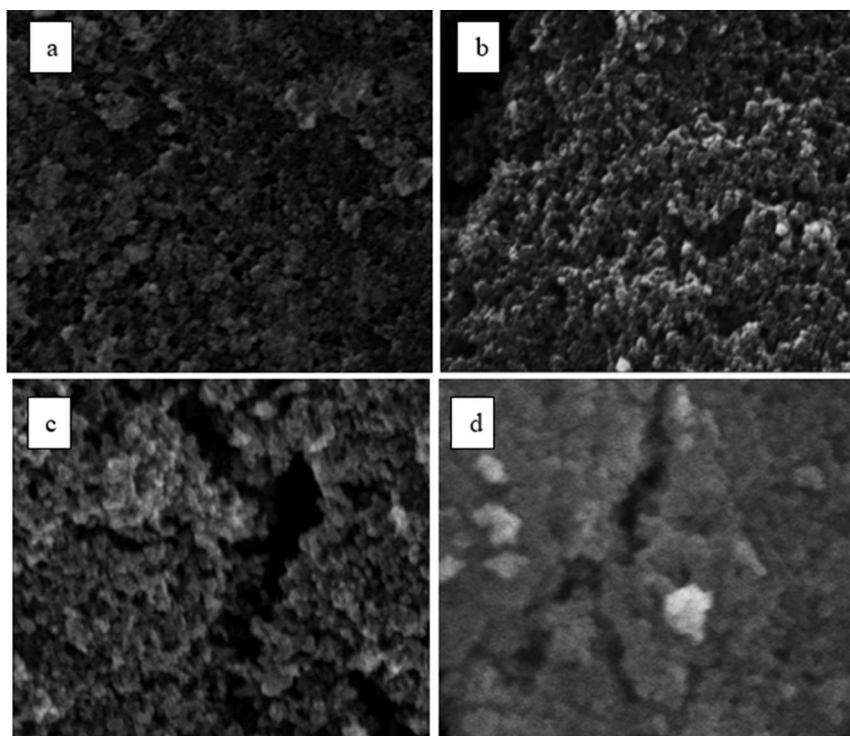Fig. 2: Three-electrode electrochemical cell.

Fig. 3: SEM images of different Sn loadings a) 3 mg.cm^{-2} b) 5 mg.cm^{-2} c) 7 mg.cm^{-2} d) 9 mg.cm^{-2}.

of the three-electrode electrochemical cell. The gas flow rate was monitored using LCD Display gas flow meter AFM0725 (Warmth Technology Co., Ltd., China). Fig. 2 shows the three-electrode electrochemical cell consisting of three electrodes.

Detection and quantification of the products: To detect and quantify the concentration of produced formic acid, UV-spectroscopy (Thermoscientific Genesys 50) was used. The concentration of formic acid was determined within the wavelength range of 200 to 250 nm, as this interval contains the most significant and characteristic peak for formic acid, which occurs specifically between 200 and 220 nm. Commercially available formic acid (AR 98%) was used as the reference.

For the CO analysis, an Arduino-based gas analyzer was employed. The gas analyzer was interfaced with an Arduino board. The collected gaseous samples were introduced into the gas analyzer in a controlled manner. A gas sensor was housed within a dedicated container, and the gas analyzer was programmed to direct the collected gas through this container. The gas sensor was sensitive to carbon monoxide and provided readings corresponding to the concentration of CO. A series of experimental runs were conducted to gather data on the change in CO(g) concentration before and after passing through the gas sensor. During each run, the gaseous byproducts collected in the gas sampling bag were introduced into the gas analyzer system for a fixed duration. Multiple experimental runs were conducted to account for variations. The calculated CO(g) concentration differences from each run were averaged to provide a representative measure of the change in CO(g) concentration due to the gas sensor's detection.

Influence of the electrolytic potential: The electrolysis conducted using the Sn GDEs produced only formic acid. No traces of CO were not detected. Conversely, in the ERC experiment done using the Zn GDE, the main product was observed to be CO., and no traces of formic acid were identified. This has good agreement with the literature (Azuma & Watanabe 1990, Hara et al. 1995, Wang et al. 2014).

To investigate the impact of different electrolytic potentials on Sn GDEs, a series of experiments were conducted using potentials of -1.1, -1.3, -1.5, -1.8, and -2 V Vs. Ag/AgCl (+0.197 Vs RHE) reference electrode. To investigate the impact of different electrolytic potentials of Zn GDEs, a series of experiments were conducted using potentials of -1.25, -1.35, -1.45, -1.55, and -1.65 V Vs Ag/AgCl reference electrodes. Each potential was applied for 30 min. The electrolyte used was 0.5 M KHCO$_3$, and CO$_2$ was fed at a flow rate of 1 dm^3·min^{-1}. The electrolyte was circulated at a constant flow rate of 21 mL.min^{-1}.

RESULTS AND DISCUSSION

Morphological Analysis of Sn GDEs and Current Efficiency Correlation

The morphologies of GDEs with different Sn loadings were observed by SEM (Fig. 3). This figure reveals that when loading increases from 3 mg.cm^{-2} to 7 mg.cm^{-2}, the number of pores between the agglomerated Sn particles has increased. As a result, the increased Sn loading allows for an enhancement in the total area of TPIs. However, with further increases in Sn loading, the number of pores decreases, leading to a subsequent reduction in the total area of TPIs.

The data presented in Fig. 4 includes the Sn loading on a gas diffusion electrode (GDE) with corresponding current density and current efficiency. As the tin loading on the GDE increases from 3 mg.cm^{-2} to 7 mg.cm^{-2}, the current density also increases. For example, at 3 mg.cm^{-2}, the current density is 0.25 mA.cm^{-2}, while at 7 mg.cm^{-2}, it increases to 0.33 mA.cm^{-2}. This trend suggests that a higher tin loading positively affects the electrochemical reduction of CO_2 by promoting higher current densities.

The increase in current density likely indicates that more active sites are available for the electrochemical reaction, leading to increased CO_2 reduction. Notably, the current efficiency also increases as the Sn loading increases. For instance, at 3 mg.cm^{-2}, the current efficiency is 18%, while at 7 mg.cm^{-2}, it rises to 36%. This implies that the higher current densities achieved at greater tin loadings are associated with higher current efficiencies.

The increase in current efficiency suggests that a larger proportion of the electrons generated during the electrochemical reaction are being utilized for CO_2 reduction. Interestingly, there is a decrease in both current density and current efficiency at an Sn loading of 9 mg.cm^{-2}. This decrease could be attributed to overcrowding of the electrode surface with tin nanoparticles, leading to reduced surface
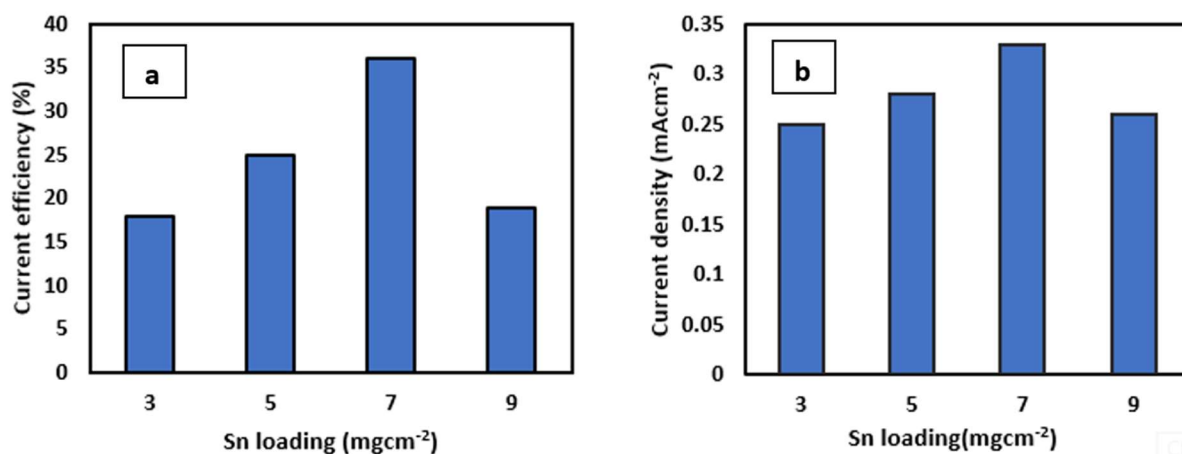

Fig. 4: The graphs of a) Current efficiency Vs. Sn loading, b) Current density Vs. Sn loading.
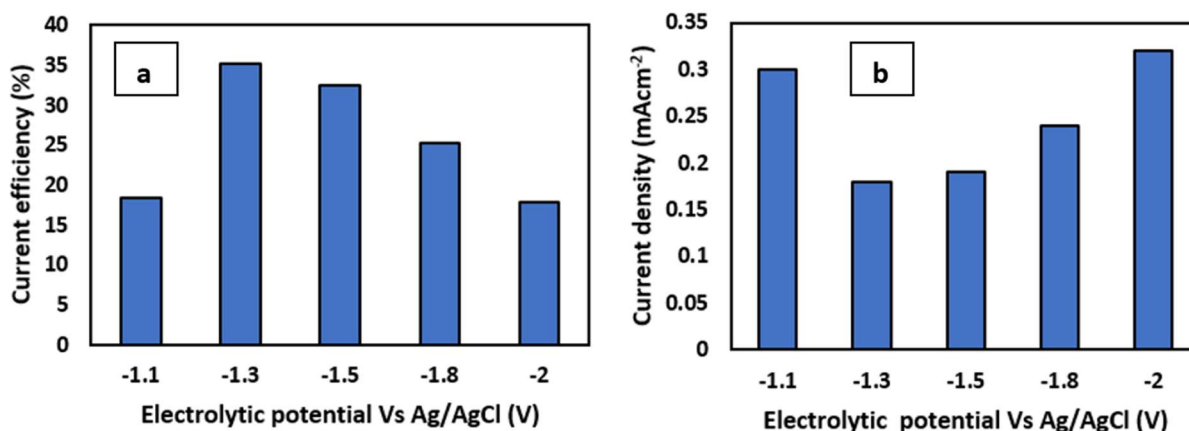

Fig. 5: The graphs of a) Current efficiency vs. electrolytic potential, b) Current density vs. electrolytic potential.

area for electrochemical reactions and potential catalyst deactivation.

Influence of Electrolytic Potential on CO_2 Conversion to Formic Acid

Fig. 5 represents the current efficiency and current density obtained in the conversion of carbon dioxide to formic with different electrolytic potentials.

At -1.1 V, the current efficiency is 14%, which steadily rises to 35% at -1.3 V. The increase in current efficiency with more negative potentials is typical in electrochemical systems. More negative potentials provide a greater driving force for the desired electrochemical reactions, resulting in higher current efficiency. The current efficiency peaks at -1.3 V (35%) and then slightly decreases at -1.5 V (31%), further decreases at -1.8 V (25%), and decreases again at -2 V (18%).

As the potential becomes more negative from -1.3 V to -2 V, the current density generally increases (Fig. 5b). The increase in current density with more negative potentials is expected due to enhanced electrode kinetics at lower potentials. As the potential becomes more negative, the electrode surface becomes more favorable for electrochemical reactions, leading to a higher rate of electron transfer and, consequently, a higher current density. However, the optimum value was suggested as -1.3 V. Analyzing the experimental data, an electrolytic potential of -1.3 V emerged as a compelling choice for optimization. This potential was suggested as the optimum value due to its combination of the highest current efficiency, the lowest current density, and the potential to minimize competing side reactions. At -1.3 V, the system exhibited exceptional efficiency, effectively channeling a significant portion of the applied current into the desired electrochemical reaction. This high current efficiency indicated a reduced occurrence of wasteful side reactions, underscoring the process's selectivity for the target product. Simultaneously, the observed low current density at this potential implied a controlled rate of electron transfer. Lower current densities can minimize competing side reactions, enhancing the efficiency of the desired electrochemical transformation. This delicate balance between selectivity, controlled electron transfer, and reduced side reactions at -1.3 V represents an optimal configuration. Such a convergence of factors not only improves the efficiency of CO_2 conversion but also extends the lifespan of electrodes, contributing to a more sustainable
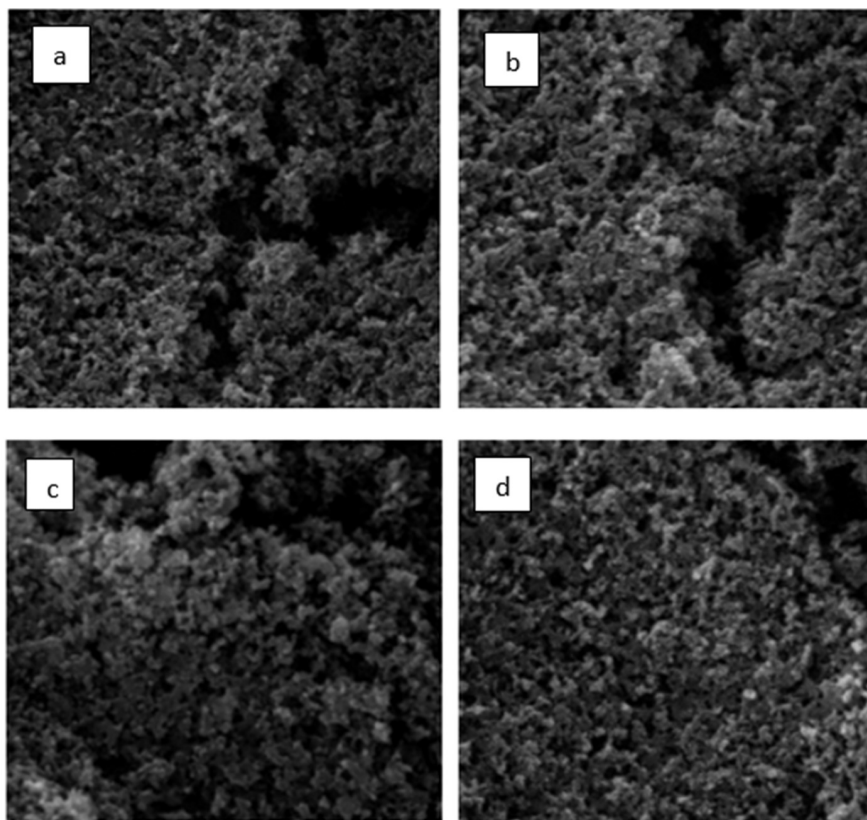

Fig. 6: SEM images of different Zn loadings a) 3 mg.cm^{-2} b) 5 mg.cm^{-2} c) 7 mg.cm^{-2} d) 9 mg.cm^{-2}.
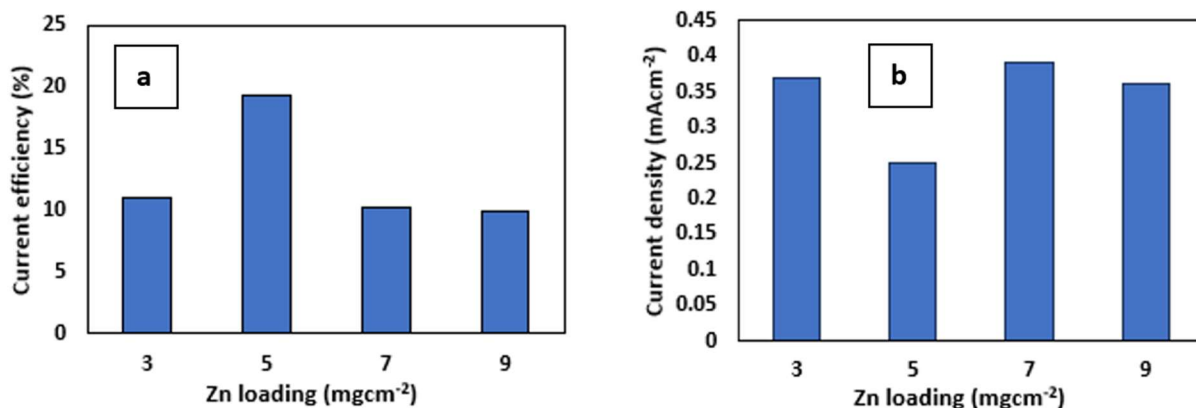
Fig. 7: The graphs of a) Current efficiency Vs. Zn loading and b) Current density Vs. Zn loading.

and cost-effective electrochemical process.

Morphological Analysis of Zn GDEs and Current Efficiency Correlation

The morphologies of GDEs with different Zn loadings were observed by SEM (Fig. 6). This figure shows that when loading increases from 3 mg.cm^{-2} to 5 mg.cm^{-2}, the number of pores between the agglomerated Zn particles increased. As a result, the increased Zn loading allows for an enhancement in the total area of TPIs. However, with further increases in Zn loading (7 and 9 mg.cm^{-2}), the number of pores decreases, leading to a subsequent reduction in the total area of TPIs.

The graphs (Fig. 7) illustrate a noticeable trend between zinc loading and current efficiency in the electrochemical system. As Zn loading varies from 3 to 9 mg.cm^{-2}, the current efficiency demonstrates a non-linear pattern. An optimum point is evident at a loading of 5 mg.cm^{-2}, where the system achieves the highest current efficiency of 19.4%. At this loading, the electrochemical system maximizes its ability to convert the applied current into the desired reaction, resulting in the highest efficiency. Deviating from this optimal loading, both lower (3 mg.cm^{-2}) and higher (7 and 9 mg.cm^{-2}) loadings result in decreased current efficiencies, indicating the presence of diminishing returns as loading diverges from the optimum. At higher loadings, mass transport limitations likely hinder the accessibility of reactants to the electrode surface, reducing the efficiency of the desired electrochemical reaction. Similarly, at lower loadings, the limited availability of active sites might lead to underutilization of the applied current, also decreasing efficiency.

The data (Fig. 7b) reveals a distinct trend where current density exhibits variations with changing Zn loading. Current density shows a fluctuating pattern with different Zn loadings. The fluctuations in current density could be attributed to the interplay between multiple factors.

The observed trend in current density can be elucidated through several electrochemical principles. Firstly, at lower Zn loadings, the active surface area available for the electrochemical reactions is limited.

Consequently, the system exhibits a relatively lower current density as there are fewer active sites for the electrochemical reactions to occur. As the Zn loading increases to 5 mg.cm^{-2}, the active surface area might become more accessible, resulting in a temporary increase in current density. However, beyond this point, the accumulation of Zn particles might start hindering mass transport, limiting the accessibility of reactants to the electrode surface and thereby decreasing the current density. This phenomenon is typical in electrochemical systems where mass transport limitations can significantly influence the observed current densities. The slight increase in current density at a Zn loading of 7 mg.cm^{-2} could be attributed to the formation of a particular surface structure that enhances the electrochemical reaction rate at this loading.

Influence of Electrolytic Potential on CO$_2$ Conversion to Carbon Monoxide

Fig. 8: represents the variation of current efficiency and current density with Electrolytic potential.

As the applied potential to the working electrode becomes more negative, moving from -1.25 V to -1.65 V, a noticeable increase in current efficiency is observed. This trend signifies that at more negative potentials, a higher percentage of electrons are efficiently utilized in the conversion of carbon dioxide to carbon monoxide. The scientific rationale behind this observation lies in the enhanced driving force for the reduction reaction at more negative potentials, reduced overpotential effects, and improved electrode kinetics. The efficiency increased from 1% at -1.25 V to a peak of 18% at -1.55 V before slightly declining to 10% at -1.65 V.
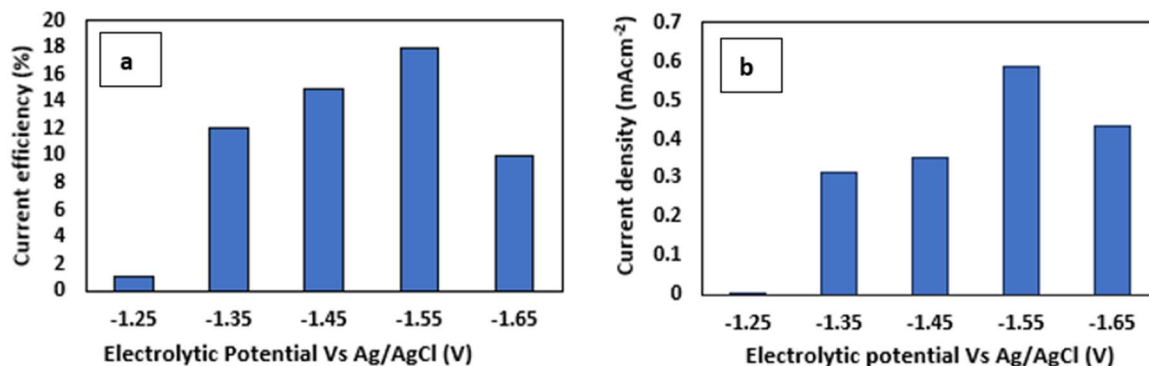
Fig 8: The graphs of a) Current efficiency vs. electrolytic potential, b) Current density vs. electrolytic potential.

The data (Fig. 8b) shows a trend where the current density initially increases with more negative potentials, reaching a peak at -1.55 V, and then decreases slightly at -1.65 V. When the electrolytic potential becomes more negative, it provides a higher driving force for the electrochemical reaction. At a more negative potential, it takes less energy for the reaction to occur, allowing a higher number of electrons to participate. This increased driving force leads to a higher rate of reaction, reflected in the rising current density up to -1.55 V. At -1.55 V, the electrochemical system reaches an optimal balance between the driving force provided by the potential and the kinetic barriers of the reaction. The reaction kinetics are favorable, meaning the reaction proceeds at an efficient rate with a high current density. Furthermore, at -1.55 V, the system achieves the highest current efficiency, indicating that a significant portion of the applied current is being utilized for the desired electrochemical reaction.

CONCLUSION

In conclusion, the experimental investigation into the electrochemical reduction of carbon dioxide to valuable chemicals, namely formic acid and carbon monoxide, has yielded valuable insights into the influence of various parameters on the efficiency of the process. In the case of Sn-loaded Gas Diffusion Electrodes (GDEs), the morphological analysis revealed a delicate balance between Sn-loading and electrochemical performance. Optimal Sn loading was found to be 7 mg.cm^{-2}, leading to increased current density and efficiency. However, excessive loading of Sn particles (9 mg.cm^{-2}) resulted in diminished performance, potentially due to overcrowding of the electrode surface. This balance highlights the importance of controlling the surface area and active sites for maximizing CO_2 reduction efficiency.

Furthermore, the choice of electrolytic potential proved to be a critical factor in determining the efficiency of CO_2 conversion. In the case of Sn GDEs, an electrolytic potential of -1.3 V Vs. Ag/AgCl emerged as the optimal choice, offering a fine-tuned balance between high current efficiency (35%) and controlled current density. This potential provided a significant driving force for the electrochemical reaction while minimizing wasteful side reactions, ensuring a selective conversion of CO_2 to formic acid. Similarly, for Zn-loaded GDEs, an optimal loading of 5 mg.cm^{-2} was identified, resulting in the highest current efficiency of 19.4%. Beyond this loading, both lower and higher loadings led to decreased efficiencies, emphasizing the importance of the active surface area in catalyzing the electrochemical reaction effectively. Regarding the electrolytic potential for Zn GDEs, the experiments revealed that a potential of -1.55 V Vs Ag/AgCl struck the perfect balance, resulting in the highest current efficiency of 18%. At this potential, the driving force for the electrochemical reaction was optimal, leading to efficient CO_2 conversion to carbon monoxide.

In summary, this study demonstrates the intricate interplay between catalyst loading, electrolytic potential, current density, and current efficiency in electrochemical CO_2 reduction. Fine-tuning these parameters is crucial for maximizing the efficiency of the process, enabling the sustainable production of valuable chemicals from carbon dioxide. These findings not only advance our fundamental understanding of electrochemical processes but also pave the way for the development of more efficient and environmentally friendly CO_2 conversion technologies.

ACKNOWLEDGMENT

REFERENCES

Azuma, M. and Watanabe, M. 1990. Electrodes in low-temperature aqueous KHCO$_3$ media. J. Electrochem. Soc., 137(6): 1772-1778.

Chen, Q., Tsiakaras, P. and Shen, P. 2022. Electrochemical reduction of carbon dioxide: Recent advances on Au-based nanocatalysts. Catalysts, 12(11): 1348. https://doi.org/10.3390/catal12111348

Del Castillo, A., Alvarez-Guerra, M., Solla-Gullón, J., Sáez, A., Montiel, V. and Irabien, A. 2015. Electrocatalytic reduction of CO$_2$ to formate using particulate Sn electrodes: Effect of metal loading and particle size. Appl. Energy, 157: 165-173. https://doi.org/10.1016/j.apenergy.2015.08.012

Del Castillo, A., Alvarez-Guerra, M., Solla-Gullón, J., Sáez, A., Montiel, V. and Irabien, A. 2017. Sn nanoparticles on gas diffusion electrodes: Synthesis, characterization, and use for continuous CO$_2$ electroreduction to formate. J. CO$_2$ Util., 18: 222-228. https://doi.org/10.1016/j.jcou.2017.01.021

Hara, K., Kudo, A. and Sakata, T. 1995. Electrochemical reduction of carbon dioxide under high pressure on various electrodes in an aqueous electrolyte. J. Electroanal. Chem., 391(1): 141-147.

Hori, Y. 2008. Electrochemical CO$_2$ reduction on metal electrodes. In Modern aspects of electrochemistry. Springer. pp. 89-189.

Hori, Y., Murata, A. and Takahashi, R. 1989. Formation of hydrocarbons in the electrochemical reduction of carbon dioxide at a copper electrode in aqueous solution. J. Chem. Soc. Faraday Trans., 85(8): 2309-2326.

Jeanty, P., Scherer, C., Magori, E., Wiesner-Fleischer, K., Hinrichsen, O. and Fleischer, M. 2018. Upscaling and continuous operation of electrochemical CO$_2$ to CO conversion in aqueous solutions on silver gas diffusion electrodes. J. CO$_2$ Util., 24: 454-462. https://doi.org/10.1016/j.jcou.2018.01.011

Kim, H.Y., Choi, I., Ahn, S.H., Hwang, S.J., Yoo, S.J., Han, J., Kim, J., Park, H., Jang, J.H. and Kim, S.K. 2014. Analysis of the effect of operating conditions on electrochemical conversion of carbon dioxide to formic acid. Int. J. Hydrog. Energy, 39(29): 16506-16512. https://doi.org/10.1016/j.ijhydene.2014.03.145

Lee, S., Ju, H.K., Machunda, R., Uhm, S., Lee, J.K., Lee, H.J. and Lee, J. 2015. Sustainable production of formic acid by electrolytic reduction of gaseous carbon dioxide. J. Mater. Chem. A, 3(6): 3029-3034. https://doi.org/10.1039/c4ta03893b

Lei, T., Zhang, X., Jung, J., Cai, Y., Hou, X., Zhang, Q. and Qiao, J. 2018. Continuous electroreduction of carbon dioxide to formate on tin nanoelectrode using alkaline membrane cell configuration in aqueous medium. Catal. Today, 318: 32-38. https://doi.org/10.1016/j.cattod.2017.10.003

Lu, X., Leung, D. Y. C., Wang, H., Leung, M. K. H. and Xuan, J. 2014. Electrochemical reduction of carbon dioxide to formic acid. Chem. Electro. Chem., 1(5): 836-849. https://doi.org/10.1002/celc.201300206

Luo, W., Zhang, J., Li, M. and Züttel, A. 2019. Boosting CO production in electrocatalytic CO$_2$ reduction on highly porous Zn catalysts. ACS Catal., 9(5): 3783-3791. https://doi.org/10.1021/acscatal.8b05109

Luo, W., Zhang, Q., Zhang, J., Moioli, E., Zhao, K. and Züttel, A. 2020. Electrochemical reconstruction of ZnO for selective reduction of CO$_2$ to CO. Appl. Catal. B Environ., 273: 119060. https://doi.org/10.1016/j.apcatb.2020.119060

Shi, R., Guo, J., Zhang, X., Waterhouse, G.I.N., Han, Z., Zhao, Y., Shang, L., Zhou, C., Jiang, L. and Zhang, T. 2020. Efficient wettability-controlled electroreduction of CO$_2$ to CO at Au/C interfaces. Nat. Commun., 11(1): 1-10. https://doi.org/10.1038/s41467-020-16847-9

Wang, Q., Dong, H. and Yu, H. 2014. Fabrication of a novel gas diffusion electrode for electrochemical reduction of carbon dioxide to formic acid. RSC Adv., 4(104): 59970-59976. https://doi.org/10.1039/c4ra10775f

Wang, Q., Wu, Y., Zhu, C., Xiong, R., Deng, Y., Wang, X., Wu, C. and Yu, H. 2021. Sn nanoparticles deposited onto a gas diffusion layer via impregnation-electroreduction for enhanced CO$_2$ electroreduction to formate. Electrochim. Acta, 369: 137662. https://doi.org/10.1016/j.electacta.2020.137662

Wu, J., Sharma, P.P., Harris, B.H. and Zhou, X. D. 2014. Electrochemical reduction of carbon dioxide: IV dependence of the faradaic efficiency and current density on the microstructure and thickness of the tin electrode. J. Power Sour., 258:189-194. https://doi.org/10.1016/j.jpowsour.2014.02.014

ORCID DETAILS OF THE AUTHORS

R. M. H. H. Jayarathne: https://orcid.org/0009-0009-4347-8112

A.R. Nihmiya: https://orcid.org/0000-0003-0903-8753

A. H. L. R. Nilmini: https://orcid.org/0000-0001-6983-2831